NANO LETTERS

2003
Vol. 3, No. 3
373−378

Two-Stage Crystal-Growth Kinetics Observed during Hydrothermal Coarsening of Nanocrystalline ZnS

Feng Huang,*,† Hengzhong Zhang,†,‡ and Jillian F. Banfield†

Department of Earth and Planetary Science, University of California, Berkeley, California 94720, and Department of Geology and Geophysics, University of Wisconsin—Madison, Madison, Wisconsin 53706

Received October 7, 2002; Revised Manuscript Received January 7, 2003

ABSTRACT

Crystal growth during hydrothermal coarsening of mercaptoethanol-capped nanocrystalline ZnS occurs via a two-stage process. In the first stage, the primary particle quickly doubles in volume. The initial growth rate can be fitted by an asymptotic curve that cannot be explained by any existing power-law dependence kinetic model developed for more coarsely crystalline material. High-resolution transmission electron microscope (HRTEM) data indicate that crystal growth within spherical nanoparticle aggregates occurs via crystallographically specific oriented attachment, despite the presence of surface-bound organic ligands. The size stabilizes for a period of time that depends on the coarsening temperature. In the second stage, following the dispersal of nanoparticles, an abrupt transition from asymptotic to cubic parabola growth kinetics occurs. The crystal growth data can be fitted by a standard Ostwald ripening volume diffusion model consistent with growth controlled by the volume diffusion of ions in solution. However, HRTEM data indicate that oriented attachment-based growth occurs in the early part of the second stage, followed by a significant reduction in aggregate surface topography, probably via surface diffusion as well as volume diffusion. We propose a new kinetic model based on oriented attachment-based growth to explain the asymptotic growth in the first stage of coarsening. The presence of surface-bound organic ligands may control the aggregation state of the nanoparticles and may permit an almost exclusive crystallographically specific oriented attachment-based growth to dominate in the first stage.

Introduction. Research on fundamental properties and behaviors of nanocrystalline ZnS has relevance to both the materials and earth sciences. The unique size-dependent properties (e.g., quantum size effects) of nanometer-scale semiconductor crystallites such as CdS, CdSe, and ZnS have been extensively studied for potential materials applications.[1] A detailed understanding of quantum size effects requires the synthesis of nanocrystals with uniform sizes and shapes.[2−4] Nanocrystalline ZnS is also formed as a product of microbial sulfate reduction in Zn-enriched environments near the earth's surface.[5] Work reported here is designed to explore crystal growth in organically capped nanocrystalline ZnS to provide insight into the fate of technologically relevant semiconductor materials at elevated temperatures and of biomineralization products over longer time scales.

An understanding of the factors that affect crystal growth kinetics and microstructure development in nanocrystals is fundamental to the control of nanoparticle properties. Typically, the kinetics of crystal growth have been studied using either micrometer-sized or nanometer-sized crystals. Existing kinetic models for coarsening are described by Ostwald ripening,[6−9] in which crystal growth is controlled by diffusion. The kinetics of crystal growth strongly depend on the structure of the material, the properties of the solution, and the nature of the interface between the crystals and the surrounding solution. Since all of the contributing factors are independent of crystal size, Ostwald ripening models assume that the crystal growth mechanism is applicable to all length scales. However, a nanocrystal is tens to thousands of times larger than a small molecule but far smaller than a macroscopic crystallite. Thus, it is possible that reactions involving nanocrystals may share some characteristics with molecular reactions in some macroscopic kinetic aspect. For example, it was shown that the nanocrystalline anatase-to-rutile phase transformation is initiated at particle−particle interfaces, [10,11] the reaction rate is controlled by the probability of nucleation at the interface between two anatase particles at temperatures below 525 °C, and the rate is second order with respect to the number of TiO_2 particles (similar to a second-order molecular reaction). As a result, the reaction rate is size-dependent.[12] The growth of nanocrystalline TiO_2 has been shown to occur primarily via oriented attachment (OA) of discrete, crystallographically oriented particles under hydrothermal coarsening conditions, a process

* To whom correspondence should be addressed. E-mail: fhuang@eps.berkeley.edu.
† University of California.
‡ University of Wisconsin—Madison.

10.1021/nl025836+ CCC: $25.00
Published on Web 02/01/2003

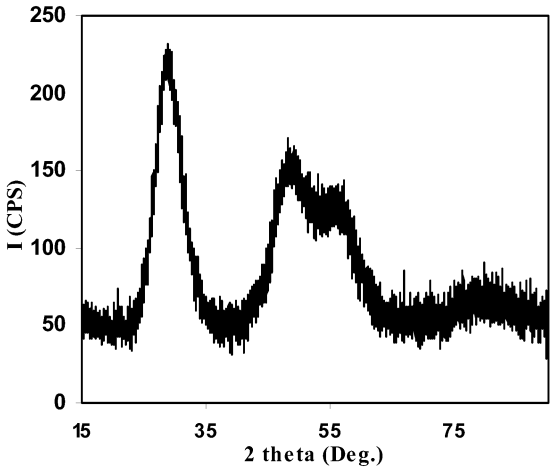

Figure 1. XRD pattern of the as-synthesized nanocrystalline ZnS (Cu Kα radiation, 0.4 °/min).

that shares characteristics with molecular reactions from the point of view that both processes produce a whole entity right after the reaction.[13] In this paper, we report a two-stage crystal growth process during hydrothermal coarsening of ZnS nanocrystalline particles with diameters of a few nanometers. A new kinetic model describing the oriented attachment (OA) of nanocrystalline ZnS particles was developed to explain the experimental results.

Experimental Section. Nanocrystalline ZnS used in this study was synthesized using Vogel's method.[14] Briefly, sodium sulfide aqueous solution was dropped into equimolar zinc chloride aqueous solution in the presence of 0.1 M mercaptoethanol at pH 10.2. Impurities were removed by dialysis treatment (until the pH was ~8.0 and Cl^- was below detection). The as-synthesized nanocrystalline ZnS particles were coarsened in aqueous solution at 140−225 °C and 3.6−25 bar in hydrothermal bombs. For time series experiments, samples of the same batch of ZnS were coarsened in separate hydrothermal vessels and sacrificed for analysis after different periods of time. X-ray diffraction (XRD) was used to identify the crystal structures and average particle sizes of as-synthesized and coarsened samples. Diffraction data were recorded using a Scintag PADV diffractometer with Cu Kα radiation (35 kV, 40 mA) in the step scanning mode. The scanning 2θ range was from 15 to 90° in steps of 0.02° with a collection time of 4 s per step. The average crystallite size was calculated using the Scherrer equation. Transmission electron microscopy (TEM) was used to confirm the particles size and determine the form of aggregates. Samples were prepared for TEM study by dispersing the ZnS powder on a holey carbon-coated Fromvar support. TEM analyses were performed using a Philips CM200 UltraTwin Electron Microscope.

Results and Discussion. Figure 1 shows the XRD pattern of the as-synthesized nanocrystalline ZnS particles that are coated and stabilized by mercaptoethanol.[14] The full width at half-maximum (fwhm) intensity of peaks (111), (220), and (311) are 3.52, 3.66, and 3.70 2θ (Cu Kα radiation), respectively. Using the Scherrer equation, the calculated average crystal dimensions perpendicular to these planes are

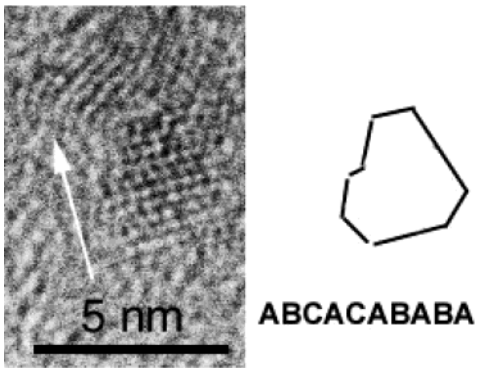

Figure 2. HRTEM image of a ZnS particle in the as-synthesized sample. The stacking sequence determined from this image is indicated to the right.

2.4, 2.4, and 2.5 nm, respectively. Thus, the as-synthesized particles are roughly equidimensional and have a diameter of 2.4 ± 0.1 nm. By comparing the experimental XRD pattern with the scattering intensities for a variety structural models of $(ZnS)_n$ calculated via the Debye function, Vogel shows that ZnS clusters synthesized by his method are a polytypic mixture of 50% sphalerite and 50% wurtzite.[14] Using the same synthesis and analysis methods, we found that the as-synthesized nanoparticles in our study consist of an intimate physical mixture of sphalerite and wurtzite but that they are dominated by the former. High-resolution transmission electron microscopy (HRTEM) observation confirmed that most of the particles are of the pure sphalerite phase (e.g., ABCABCAB stacking sequence). Figure 2 shows a specific HRTEM image of a ZnS particle where the close-packed layer-stacking sequence in the direction indicated by the arrow is ABCACABABA.

Suspensions of coarsened material from kinetic experiments carried out in water at 140, 175, 200, and 225 °C were dropped onto a low-background holder (made from a single crystal of quartz; SiO_2) for XRD characterization. Figure 3a−d shows the increase in average particle sizes versus time at each temperature. In each case, crystal growth occurs in two stages: In the first stage, the particle grows rapidly to a limiting size of about 3.1 nm, after which growth essentially ceases for a period of time that depends on the reaction temperature. In the second stage, crystal growth is reinitiated but at a rate that is slower than the initial rate in the first stage.

Existing models can be used to describe coarsening during the second stage. The growth of individual crystals of average particle diameter, D, dispersed in a homogeneous matrix can be described by an equation for Ostwald ripening:[7]

$$D - D_0 = kt^{1/n} \tag{1}$$

where t is time, k is a temperature-dependent material constant appropriate to the value of the exponent n, and D_0 is the average particle diameter at $t = 0$. When the exponent n is equal to 2, it is inferred that crystal growth is controlled by the diffusion of ions along the matrix−particle boundary; when $n = 3$, the growth is controlled by the volume diffusion

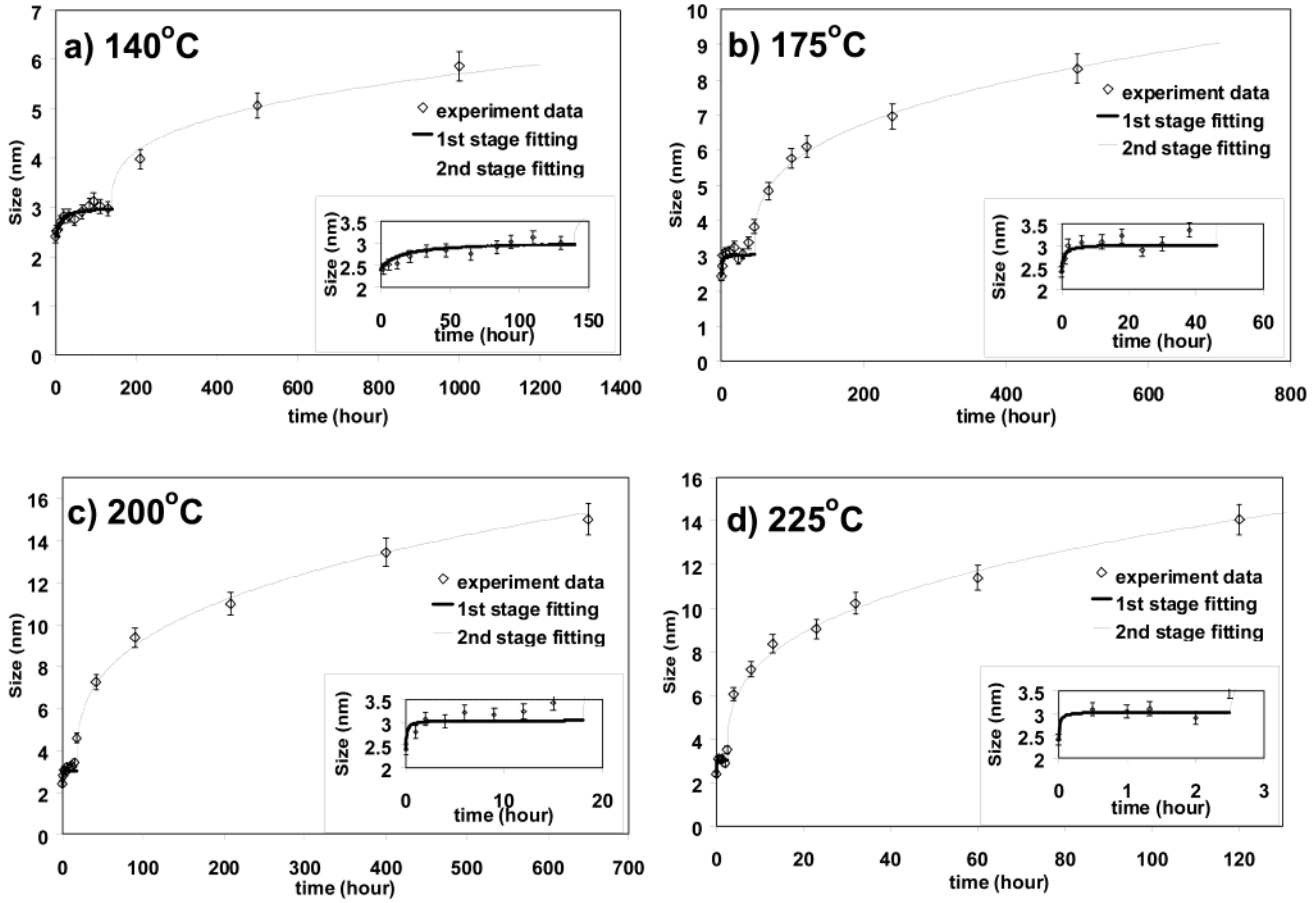

Figure 3. Experimental data and fitting results showing particle size vs time at each temperature; insets are enlarged plots for the first stage of coarsening.

Table 1. Least-Square Fitting Parameters at Each Temperature

T (°C)	$D_0{}^a$ (nm)	$k_1{}^a$ (hours^{-1})	$D_2{}^b$ (nm)	$1/n^b$	t_2 (hours)	$k_2{}^b$ (hours$^{-1/3}$)
140	2.43	0.07	3.34	0.328	140.12	0.2818
175	2.45	1.58	3.22	0.333	46.03	0.6924
200	2.40	11.0	3.17	0.335	17.96	1.432
225	2.37	63.7	3.21	0.317	2.50	2.253

[a] For the first stage. [b] For the second stage.

of ions in the matrix; and when $n = 4$, it is deduced that growth is controlled by dissolution kinetics at the particle−matrix interface.[7−9] The second stage of crystal growth in our experiments can be fitted well to eq 1, where D_2 and t_2 are the starting size and time, respectively, to be determined by the fit. Thus, the fitting equation should be

$$D - D_2 = k(t - t_2)^{1/n} \qquad (2)$$

Table 1 shows the fitting results. The values of D_2 and n are almost same for each temperature, but t_2 decreases rapidly with increasing temperature. The fitted result for the starting average particle diameter ($D_2 = 3.17-3.34$ nm) at the beginning of stage two matches well with the growth limit of the first stage for each temperature (~3.1 nm). $n \approx 3$ suggests that the kinetics of the second stage are controlled by the volume diffusion of ions in the solution.[7] The consistency of results for the second stage implies that after crystal growth is reinitiated following the first stage, the growth-control factors for the first stage have little influence. (Figure 3)

Fitting of the first stage of growth using eq 1 yielded an exponent of $n > 10$. Such a large exponent bears no physical meaning. Thus, a new kinetic model is required to explain the experimental results. Just as OA can occur in the hydrothermal coarsening of nanocrystalline TiO_2, we find that very small ZnS nanocrystals can grow via oriented attachment (OA). Figure 4A shows a HRTEM image of a ZnS sample coarsened at 225 °C for 0.5 h: three small particles attached to a central particle were observed. The grain edges are illustrated in Figure 4B. In the present work, a new size-dependent kinetic model for nano-ZnS growth via OA is developed to explain the kinetics of particle growth in the first stage.

In OA-based coarsening, two small nanoparticles combine to form a larger particle without the dissolution of either particle. Thus, growth via OA is controlled by the probability of contact between nanoparticles in appropriate orientations, as for interface nucleation of the phase transformation in nanocrytalline TiO_2.[15] By analogy, we suggest that the OA-based growth of nanocrystals is related to the number of

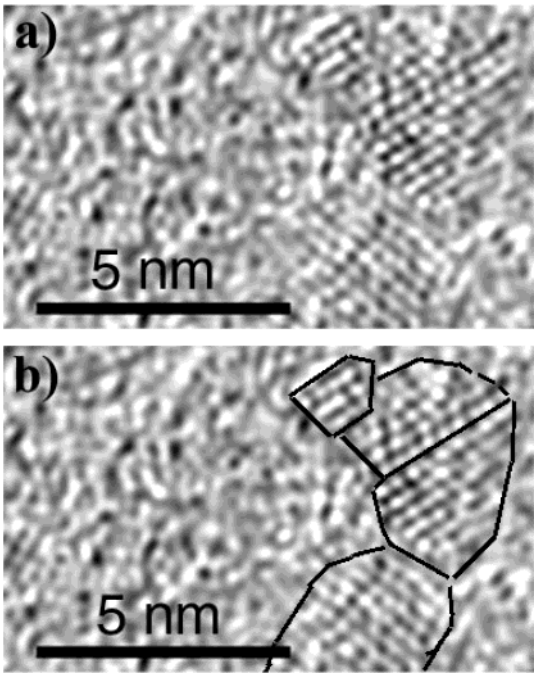

Figure 4. (A) HRTEM image of four attached ZnS particles (hydrothermal coarsening at 225 °C for 0.5 h). (B) HRTEM image in part A with lines to indicate the shape and interface positions.

initial particles in a given volume (i.e., the "concentration" of nanoparticles).

During stage one, the particle size increases from 2.4 to 3.1 nm. Assuming that the particles are approximately spherical, we can calculate that the average volume of a grown particle, V_2, is about double the average initial volume, V_0, of an initial ZnS particle. This suggests that the primary reaction during stage one involves a combination of Zn and S atoms from two ZnS particles to form one ZnS particle, a reaction that is consistent with crystal growth via oriented attachment.

Suppose that the initial average particle size and number are, respectively, D_0 and N_0 at $t = 0$. After growth via oriented attachment for a period of time t, the number of initial particles is $N(t)$, and the number and the average particle size of grown particles are $N_2(t)$ and D_2, respectively. According to the principle of mass balance,

$$\frac{1}{6}\pi\rho {D_0}^3 N_0 = \frac{1}{6}\pi\rho {D_0}^3 N(t) + \frac{1}{6}\pi\rho {D_2}^3 N_2(t) \tag{3}$$

where ρ represents the density of ZnS. Since $V_2 = 2V_0$, $D_2 = \sqrt[3]{2}D_0$, and we have

$$N_2(t) = (N_0 - N(t))/2 \tag{4}$$

The oriented attachment rate, the number of initial particles reacted in a unit time, can be written as

$$-\frac{\mathrm{d}N(t)}{\mathrm{d}t} = kN(t)^2 \tag{5}$$

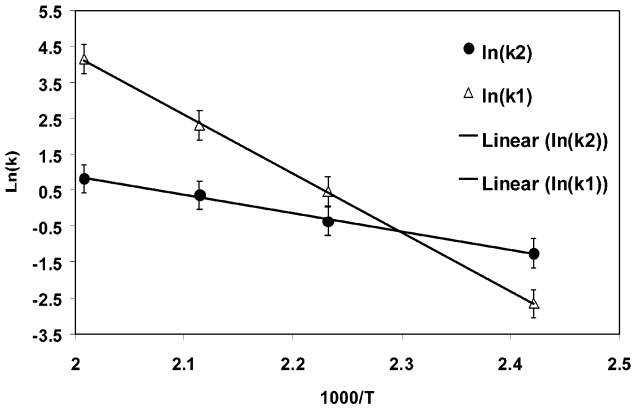

Figure 5. Arrhenius plot of the two kinetic constants.

By integrating eq 5, we have

$$\frac{1}{(N(t)/N_0)} = k_1 t + 1 \tag{6}$$

where $k_1 = kN_0$.

According to the definition of the volume-weighted average particle size,[16] which is consistent with the average particle size determined by XRD using the Scherrer method, the average particle size D in the first stage can be related to D_0 and D_2 by

$$D = \frac{N(t){D_0}^4 + N_2(t){D_2}^4}{N(t){D_0}^3 + N_2(t){D_2}^3} \tag{7}$$

Combining eqs 7, 6, and 4, we have

$$D = \frac{D_0(\sqrt[3]{2}k_1 t + 1)}{(k_1 t + 1)} \tag{8}$$

The first stage of crystal growth can be fitted well using eq 8 with D_0 and k as least-squares fitting parameters. Table 1 and Figure 3 show the fitted results for the four temperatures.

Phenomenological kinetic analysis shows that the coarsening process of mercaptoethanol-stabilized ZnS nanoparticles exhibits two stages with different growth mechanisms. So far, kinetic constants were obtained for the two coarsening stages (Table 1). Their temperature variation can be described by the Arrhenius equation

$$\ln k = -\frac{E_a}{RT} + A_0 \tag{9}$$

where E_a is the activation energy, A_0 is the preexponential factor, R is the universal gas constant, and T is the absolute temperature. From the Arrhenius plot of various kinetic constants (Figure 5), we obtained the activation energy of oriented attachment $E_a(k_1) = 136.8 \pm 9.1$ kJ/mol and the activation energy of Ostwald ripening $E_a(k_2) = 41.8 \pm 5.9$

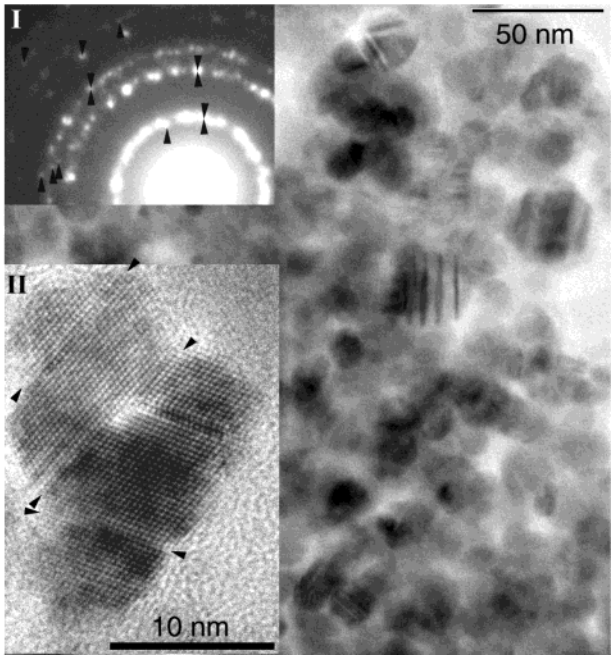

Figure 6. HRTEM image of larger ZnS particles (hydrothermally coarsened at 225 °C for 4 h). Inset I: electron diffraction pattern of this area. Inset II: HRTEM of at least five attached ZnS particles. Arrowheads mark some interfaces between primary particles.

kJ/mol. The standard deviation was estimated from the deviation between ln k and the fitting in Figure 5 using eq 9.

The kinetic analysis, in combination with TEM data, indicates that in the temperature range of 140−225 °C nanocrystalline ZnS particle growth is initially dominated by oriented attachment. Kinetic data for the second stage are consistent with growth via Ostwald ripening. However, OA may also occur in the prophase of the second stage and even may predominate if OA kinetics adopt a form similar to Ostwald ripening. Phenomenological kinetic analysis shows that hydrothermal coarsening ZnS sample at 225 °C for 4 h is dominantly grown through Ostwald ripening. However, HRTEM observations indicate both Ostwald ripening growth and OA growth. Figure 6 shows the large-scale HRTEM image of this sample. Many Ostwald ripening (round shape with a smooth edge) and OA (irregular shape with an abrupt edge) particles can be found in this image. Inset II shows a group of four attached particles with clear grain edges and the same orientations, and arrowheads mark interfaces between primary particles. Inset I shows the electron diffraction pattern of the large-scale area. With the increase of the coarsening time, the action of OA growth becomes smaller and smaller. In the HRTEM images of the hydrothermally coarsening ZnS sample at 225 °C for 32 h, no OA growth particles can be found (data are provided elsewhere—Huang et al., in preparation).

The two-stage kinetics of the coarsening process may be explained by the aggregation state of the nanoparticles in the starting materials.TEM images of the as-synthesized sample and the sample coarsened for 0.5, 4, and 32 h at 225 °C are shown in Figure 7. The nanoparticles in the as-synthesized and 0.5-h samples are aggregated into balls of 0.3−2 μm radius, whereas nanoparticles in samples coarsened for 4 and 32 h are dispersed. The initial 2.4-nm particles

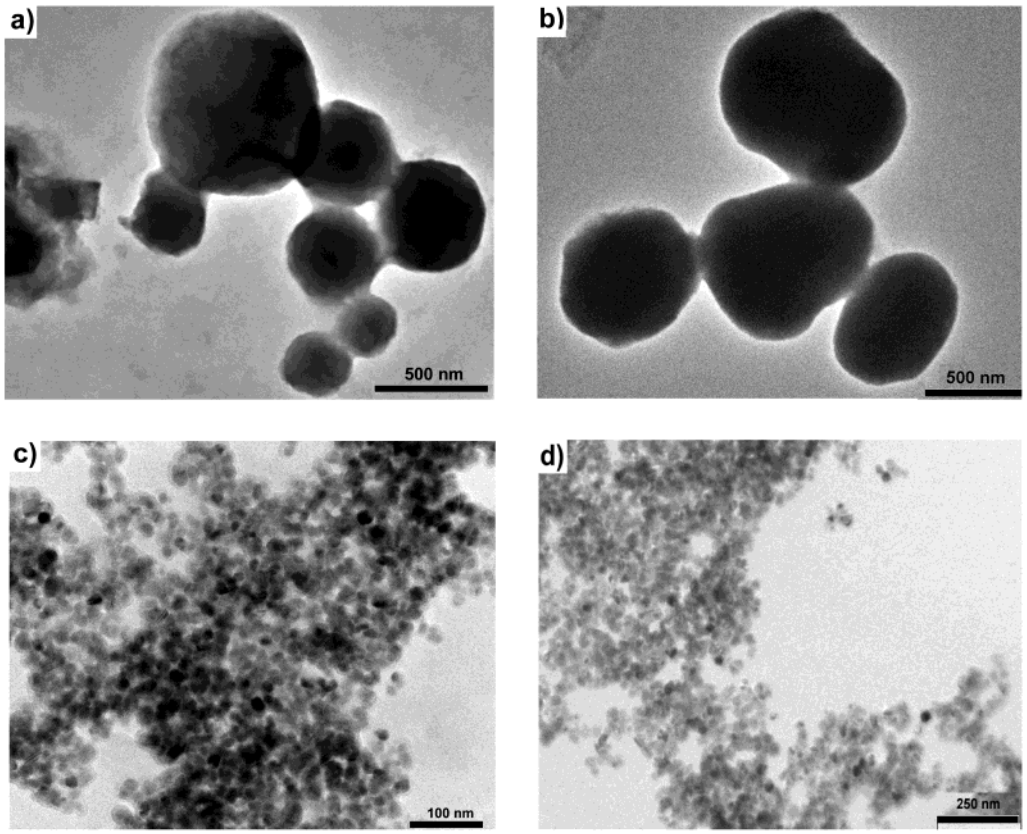

Figure 7. TEM images of samples coarsened at 225 °C for (a) 0 h (as-synthesized sample), (b) 0.5 h, (c) 4 h, and (d) 32 h.

are coated and stabilized by mercaptoethanol,[14] which appears to favor aggregation (Figure 7a and b). At the beginning of the hydrothermal reaction, the mercaptoethanol coating on ZnS nanoparticles could have prevented particle coarsening by inhibiting the diffusion of ions by the elimination of water molecules. Aggregation ensures small distances between the nanoparticles, providing the possibility of coarsening via oriented attachment as the organic ligands desorb. Once a particle−particle pair is formed, the radius of the new larger particle is smaller than twice the radius of the two primary particles. As a consequence, the distance between the new particle and other adjacent particles will increase.

Experimental results show that after the oriented attachment the particle growth essentially ceased for a certain period of time, the length of time being inversely dependent on temperature. It is probable that during this stage the mercaptoethanol molecules coating the surface will be replaced by H_2O molecules. Eventually, the spherical aggregates disperse (Figure 7c and d). This phenomenon appears to correspond to the onset of growth in stage two.

In stage two, the presence of water surrounding the nanoparticle surfaces induces oriented attachment because water molecules can enhance Brownian motion-induced reorientation and promotes growth by bulk diffusion. Diffusion, either via surface reorganization or the addition of ions from aqueous solution, eliminates the indents at particle contacts, ultimately generating rounded crystals. These crystals contain defects such as stacking faults and twins that are a legacy of their oriented attachment-based growth history.

In conclusion, the coarsening of mercaptoethanol-stabilized ZnS nanoparticles can be divided into two stages. The two-stage growth kinetics are primarily attributed to the presence of organic ligands, which control the aggregation state of the nanoparticles. In the first stage, the particle volume doubles. Our results show that despite the presence of adhering organic molecules, coarsening is controlled by oriented attachment. This finding has important implications for biomineralization and biomimetic processes in which large single crystals with distinctive morphologies may be assembled from nanoparticle components. After the first stage, growth ceases until surface-bound ligands are removed, at which point growth can be fitted by a bulk diffusion Oswald ripening model, despite the fact that growth occurs simultaneously by oriented attachment and Ostwald ripening. The time required for ligand removal and nanoparticle dispersal (the beginning of stage two) is determined by the temperature. As particle size increases, oriented attachment-based growth becomes less important. Sphalerite (ZnS) has higher symmetry than many other compounds for which OA has been documented previously (TiO_2,[13] FeOOH,[17] CoOOH[18]). Because particles are bounded by four {111} faces, the adoption of orientations consistent with the formation of a coherent {111} interface may be especially probable.

Acknowledgment. Financial support for this study was provided by National Science Foundation Grant EAR-9814333 and the Department of Energy Basic Energy Sciences Program Grant DE-FG03-01ER15218. Transmission electron microscope characterization was conducted in the Materials Science Center, University of Wisconsin—Madison. Mr. Michael Finnegan provided assistance with the use of hydrothermal and XRD equipment.

References

(1) Alivisatos, A. P. *J. Phys. Chem.* **1996**, *100*, 13226.
(2) Efros, Al. L.; Efros, A. L. *Sov. Phys. Semicond.* **1982**, *16*, 772.
(3) Ekimov, A. I.; Onushchenko, A. A. *Sov. Phys. Semicond.* **1982**, *16*, 775.
(4) Brus, L. E. *J. Chem. Phys.* **1983**, *79*, 5566.
(5) Labrenz, M.; Druschel, G. K.; Thomsen-Ebert, T.; Gilbert, B.; Welch, S. A.; Kemner, K. M.; Logan, G. A.; Summons R. E.; Stasio, G. D.; Bond, P. L.; Lai, B.; Kelly, S. D.; Banfield, J. F. *Science (Washington, D.C.)* **2000**, *290*, 1744.
(6) Lu, K. *Mater, Sci. Eng.* **1996**, *R16*, 161.
(7) Kirchner, H. O. K. *Metall. Trans.* **1971**, *2*, 2861.
(8) Speight, M. V. *Acta Metall.* **1968**, *16*, 133.
(9) Wagner, C. *Z. Elektrochem.* **1961**, *65*, 581.
(10) Penn, R. L.; Banfield, J. F. *Am. Mineral.* **1999**, *84*, 871.
(11) Penn, R. L.; Banfield, J. F. *Geochim. Cosmochim. Acta* **1999**, *63*, 1549.
(12) Zhang, H.; Banfield, J. F. *Am. Mineral.* **1999**, *84*, 528.
(13) Penn, R. L.; Banfield, J. F. *Science (Washington, D.C.)* **1998**, *281*, 969.
(14) Vogel, W.; Borse, P. H.; Deshmukh, N.; Kulkarni, S. K. *Langmuir* **2000**, *16*, 2032.
(15) Zhang, H.; Banfield, J. F. *J. Mater. Res.* **2000**, *15*, 437.
(16) Allen, T. *Particle Size Measurement*; Chapman and Hall: New York, 1997; Vol. 1, p 53.
(17) Penn, R. L.; Oskam, G.; Strathmann, G. J.; Searson, P. C.; Stone, A. T.; Veblen, D. R. *J. Phys. Chem. B* **2001**, *105*, 2177.
(18) Penn, R. L.; Stone, A. T.; Veblen, D. R. *J. Phys. Chem. B* **2001**, *105*, 4690.

NL025836+